Chinese Chemical Letters 32 (2021) 539–542

Contents lists available at ScienceDirect

Chinese Chemical Letters

journal homepage: www.elsevier.com/locate/cclet

Communication

High-temperature dielectric switch and second harmonic generation integrated in a stimulus responsive material

Yingsong Xue, Zhixu Zhang, Pingping Shi, Wanying Zhang, Qiong Ye*, Dawei Fu*

Ordered Matter Science Research Center, Jiangsu Key Laboratory for Science and Applications of Molecular Ferroelectrics, Southeast University, Nanjing 211189, China

ARTICLE INFO

Article history:
Received 10 December 2019
Received in revised form 31 January 2020
Accepted 5 February 2020
Available online 6 February 2020

Keywords:
Dielectric switch
Second harmonic generation
High-temperature
Phase transition
Stimulus responsive material

ABSTRACT

Stimulus responsive materials can provide a variety of desirable properties in one equipment unit, such as optoelectronic devices, data communications, actuators, memories, sensors and capacitors. However, it remains a large challenge to design such stimulus responsive materials, especially functional materials having both dielectric switch and second harmonic generation (SHG). Here, a new stimuli-responsive switchable material $[(CH_3)_3N(CH_2)_2Cl]_2[Mn(SCN)_4(H_2O)_2]$ was discovered as a potential second-harmonic generation (SHG) dielectric switch. It is worth noting that it has SHG characteristics before and after undergoing reversible high-temperature phase transitions. In this work, we successfully refined the tetramethylammonium cation to obtain a *quasi*-spherical cation, which is tetramethylchloroethylamine (TMCEM) cation. By substituting H with a halogen, the increased steric hindrance of the molecular makes energy barrier increased, resulting in the reversible high-temperature phase transition. At the same time, the interactions of quasi-spherical cations and $[Mn(SCN)_4(H_2O)_2]^{2-}$ anions affect a non-centrosymmetric structure to induce the SHG effect. These findings provide a new approach to design novel functional switch materials.

Smart response and information processing have been an important issue related to the living and daily production of human being [1–3]. Stimulus responsive materials that can make corresponding signal actions in response to external stimuli have recently attracted much attention, especially dielectric switch and nonlinear optical effects [4–7]. Such materials have widespread applications such as optoelectronic devices, data communications, actuators, memories, sensors and capacitors, *etc.* [8–13]. For these materials, it is crucial to explore the relationship between properties and structure, and various methods have been used to design these functional materials [14–18]. From the perspective of crystallographic engineering analysis, the slightly changes in microstructure of the crystal can make the variation of the physical/chemical properties in different conditions, and thereby resulting in some desired performances such as switchable, magnetic, optoelectronic and ferroelectricity [19–22]. However, it remains a large challenge to design such stimulus responsive materials, especially functional materials having both dielectric switch and second harmonic generation (SHG).

Exploring reasonable methods to design responsive switchable materials have always been intriguing and urgent. Constructing inorganic–organic hybrid materials afford an important opportunity to integrate phase transition with SHG effect, because hybrids can combine the advantages of both inorganic frameworks and organic molecules to achieve multifunctional characteristics, compared to some pure organic or inorganic compounds [23–27]. Our colleagues discovered an inorganic–organic hybrid perovskite ferroelectric $[(CH_3)_3NCH_2Cl]MnCl_3$ [28], which experienced a reversible phase transition that caused by the order-disorder transition of $[(CH_3)_3NCH_2Cl]^+$ cation, exhibiting large piezoelectric response comparable with piezoceramics such as barium titanate. The $[(CH_3)_3NCH_2Cl]^+$ cation is obtained by modifying the tetramethylamine cation, which is based on the "*quasi*-spherical theory" recently proposed by our group: the modification of spherical cations into a quasi-spherical cation [29]. Specifically, a specific chemical group is introduced into the spherical tetramethylamine cation to construct a quasi-spherical cation, thereby causing a change in molecular symmetry and dipole moment. By reducing its symmetry and increasing its kinetic energy barrier, high temperature phase transition, large piezoelectric, ferroelectric and other excellent properties are obtained. Based on this theory, there are many excellent stimuli-responsive solid materials that we get: $[Me_3NOH]_2[KFe(CN)_6]$ [27],

* Corresponding authors.
E-mail addresses: yeqiong@seu.edu.cn (Q. Ye), dawei@seu.edu.cn (D. Fu).

https://doi.org/10.1016/j.cclet.2020.02.005

$[Me_3NCH_2X]MnX_3$ (X = Cl^-, Br^-) [28,30], $[Me_3NCH_2I]PbI_3$ [31], [Mdabco]NH_4X_3 (X = Br^-, I^-) (Mdabco = *N*-methyl-*N*′-1,4-diazoniabicyclo[2.2.2]octonium) [6], [Mdabco]RbI_3 [32], and [Odabco]NH_4X_3 (X = Cl^-, Br^-) (Odabco = *N*-hydroxy-*N*′-1,4-diazoniabicyclo [2.2.2]octonium) [6]. Reducing its symmetry can change the dipole moment to obtain SHG. Replacing H with halogens increases the kinetic energy barrier and may be an excellent way to increase/get high phase transition temperatures. In addition, we have found a dielectric switch functional material $[(CH_3)_4P]_4[Mn(SCN)_6]$, which has two consecutive phase transitions which are related to the motion of $[Mn(SCN)_6]^{4-}$ anion and $[(CH_3)_4P]^+$ cations [33–35]. By summarizing the previous work, we noticed that the configuration changes and the motion of the thiocyanate anion are prone to phase transitions, which is related to the momentum matching theory. The intermolecular interactions of the cation and anion are particularly crucial for affecting the crystal structure to reasonably induce phase transition and SHG effect.

Inspired by this strategy, we successfully refined the tetramethylammonium cation to obtain a *quasi*-spherical cation, that is tetramethylchloroethylamine (TMCEM) cation. We assembled (2-chloroethyl) trimethylammonium chloride, potassium thiocyanate, and manganese(II) nitrate hexahydrate to design a new responsive switchable material $[(CH_3)_3N(CH_2)_2Cl]_2[Mn(SCN)_4(H_2O)_2]$ (compound **1**), which exhibits a high-temperature phase transition at 371 K with SHG effect. By substituting H with a halogen, the increased steric hindrance of the molecular make energy barrier increased, resulting in the reversible high-temperature phase transition. At the same time, the interactions of quasi-spherical cations and $[Mn(SCN)_4(H_2O)_2]^{2-}$ anions affect a non-centrosymmetric structure to induce the SHG effect.

It is well known that there are a number of characterization methods that can be used as evidence of phase change because physical properties such as magnetic properties and dielectric properties may change. In these measurements, DSC measurement is one of the most effective methods to determine whether this compound goes through a reversible phase transition triggered by thermal stimulate (Fig. 1 and Fig. S1 in Supporting information). In addition, thermogravimetric (TG) analysis indicate that the compound shows good thermal stability (Fig. S2 in Supporting information). As show in Fig. 1, DSC measurements were performed at a temperature range of 313–385 K. Underneath a liquid nitrogen atmosphere, the crystalline samples (9.1 mg) were heated and cooled with a rate of 10 K/min. One pair of endothermic and exothermic peaks were detected at 347.8/371.0 K in the heating and cooling runs, respectively, indicative of a reversible structural phase transition. The sharp shape of these peaks and the thermal hysteresis reveal a first-order phase transition. On the basis of DSC curves, the average entropy change (ΔS) was calculated to be ~18.32 J mol^{-1} K^{-1}. In the Boltzmann equation $\Delta S = R \ln(N)$, *R* is the gas constant, *N* is the ratio of the quantity of individual geometrically distinguishable orientations, and the value of N is calculated to be 9.06. For the purposes of the following explanation, the phase below T_c is labeled as the low temperature phase (LTP) and the phase above T_c is labeled the high temperature phase (HTP).

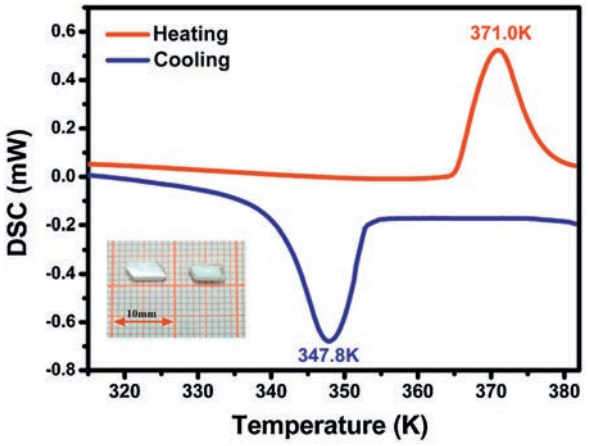

Fig. 1. DSC curves of **1** in the heating and cooling runs at the first cycle. Insert: Single-crystal samples of **1**.

For analysis of the microscopic mechanism of the reversible phase transition, Single-crystal X-ray structure determinations were performed on compound **1**. At 293 K, compound **1** crystallized in the monoclinic space group *Cc* (No. 9), with cell parameters of *a* = 26.0997(12) Å, *b* = 7.4703(4) Å, *c* = 14.3438(8) Å, β = 102.290 (5) ° and *V* = 2732.6(2) $Å^3$. In the LTP, the asymmetric unit contains two TMCEM cations and a $[Mn(SCN)_4(H_2O)_2]^{2-}$ anion (Fig. 2a). For metal skeleton anions, the coordination geometry of the central Mn atom consists of two coordinating H_2O molecule and four SCN^- anions in which the N atoms are linked to Mn atom. Symmetry site of each Mn atom lies in the glide plane with the Mn–N bond distances varied from 2.153(9) Å to 2.234(8) Å, and the Mn–O bond distances are 2.211(6) and 2.200(7) Å (Table S1 in Supporting information). The O–Mn–O bond angle is 178.2(4)° and the O–Mn–N bond angles are in range from 88.7(3)° to 92.9(3)°. The vertical N–Mn–N bond angles are varied from 89.0(3)° to 91.9° while the opposite N–Mn–N bond angles are 177.3(5)° and 179.2 (5)°, respectively. From above bond distances and angles, N and O atoms are coordinated with central Mn atom to form a slightly distorted octahedron configuration. There are four Mn–N–C–S torsion angles range from 121(15)° to 163(17)°. Notably, different from common $Mn(SCN)_3$, the coordination environment of Mn atom changed to construct a rare metal skeleton structure in which water molecules participate in coordination, owing to the influence of *quasi*-spherical cations formed by introducing chloromethyl group into tetramethylamine cation.

From packing structure, TMCEM cations are loosely connected to the Mn-based anionic framework by weak forces to form a zero-dimensional topological structure (Figs. 2b and Fig. S4 in Supporting information). Interestingly, $[Mn(SCN)_4(H_2O)_2]^{2-}$ anions are also loosely connected to each other by intermolecular hydrogen bond (O–H···S, distances from 2.44 Å to 2.75 Å) parallel to the bc plane, resulting in a two-dimensional-like crystal structure (Fig. 2c). The TMCEM cations are located in the cavities between the two-dimensional-like metal skeletons that joined by hydrogen bonds. The cavities provide spaces of cationic motion, offering the opportunity for possibility of reversible phase transition.

The single-crystal structure in HTP has not been successfully determined due to few or even indistinguishable peaks with relatively weak intensity, especially for those in the relatively high-angle region. Even so, variable-temperature powder X-ray diffraction (PXRD) measurements can be further confirm and provide some information about the phase transition of $[(CH_3)_3N(CH_2)_2Cl]_2[Mn(SCN)_4(H_2O)_2]$. To further confirm the existence of the reversible phase transition at HTP, compound **1** was subjected to variable temperature PXRD measurement. As shown in Fig. S5 (Supporting information), the PXRD pattern obtained at 293 K exactly matches the corresponding simulation result (bottom line) recorded from the single crystal structure. When the temperature increased to 363 K, however, obvious changes have been recorded in comparison with the patterns at LTP. For instance, the diffraction peaks at 12.31°, 12.62°, 13.49°, 13.87°, 14.19°, 16.16°, 16.67°, 17.81°, 18.20° and 18.79° disappeared in the LTP, while five new diffraction peaks were observed at 7.91°, 8.85°, 11.31°, 14.83° and 17.97° in the HTP. Compared with 5°–20°, there are more obvious diffraction peaks between 20°–30°, and the four distinct diffraction peaks of 21.56°, 22.08°, 23.02° and 23.76° have not changed. However, the

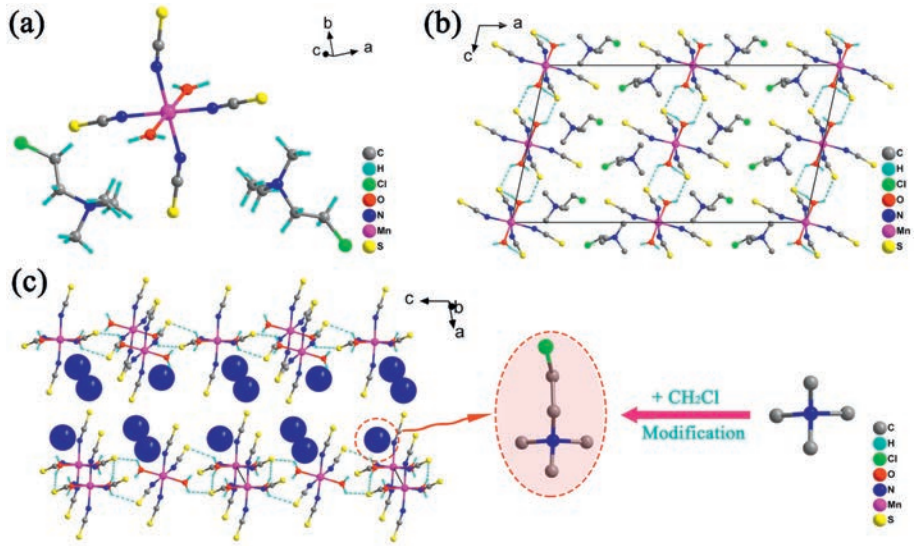

Fig. 2. (a) The asymmetric unit structure of compound **1**. (b) Packing view of compound **1** along *b* axis. (c) The schematic diagram of two-dimensional-like structure.

five diffraction peaks at 24.64°, 24.85°, 25.25°, 25.40° and 25.85° disappeared, and the two diffraction peaks at 26.49° and 26.72° became a diffraction peak of 26.68°. In addition, the three diffraction peaks of 27.23°, 27.78°, and 28.15° emerged in LTP, and two new diffraction peaks appeared in the corresponding HTP at 27.38° and 28.72°. There are some minor diffraction peaks around 32° and 35°, the small diffraction peak around 40° increased to a more obvious large diffraction peak. In addition, to further explore the structural changes of **1**, the PXRD data at 363, 378 and 388 K were simulated with the Materials Studio program (Fig. S7 in Supporting information). The indexing of the PXRD patterns reveal a tetragonal unit cell and the Pawley refinements reveal a possible point group 4/*mmm*, among which, the most possible space group is the *I*4/*mmm*. In general, significant changes in the PXRD pattern strongly confirm the existence of phase transitions, and the sharp decrease in diffraction peaks is relevant to the transition from low symmetry to high symmetry.

We further confirm the non-centrosymmetric nature of the crystal structures of compound **1** by the second harmonic generation (SHG) measurements. As shown in Fig. 3, compound **1** exhibits obvious SHG responses with non-zero SHG intensities at room temperature, revealing the crystal symmetry of compound **1** is non-centrosymmetric. With the temperature increased, the SHG intensities of compound **1** keep stable from LTP to HTP, which indicates compound **1** also locates in a non-centrosymmetric point group in HTP, consistent with the crystal analysis and PXRD results. Due to the unique crystal structure, the nature of non-centrosymmetric structure can be maintained in both LTP and HTP.

The dielectric constant ε is an important physical property of materials, which can act as a signal to sensitively detect structural phase transitions as a result of local polarization changes. There is a dielectric constant formula $\varepsilon = \varepsilon' - i\varepsilon''$, where ε' is the real part and ε'' is the imaginary part. The temperature-dependent dielectric properties were measured on polycrystalline sample of compound **1** in the temperature range of 320–380 K at 1 MHz. The temperature-dependent dielectric constant of compound **1** is shown in Fig. 4. During the heating-cooling process, the exothermic and endothermic peaks emerge at 355 K and 370 K, respectively, which is consistent with the DSC results and conform to phase transition of the crystal. The real part of the dielectric constant ε' is maintained at about 10 at room temperature and then rapidly increases to 22 at around 365 K. The value of ε' in the high temperature state rises to more than twice that in the low

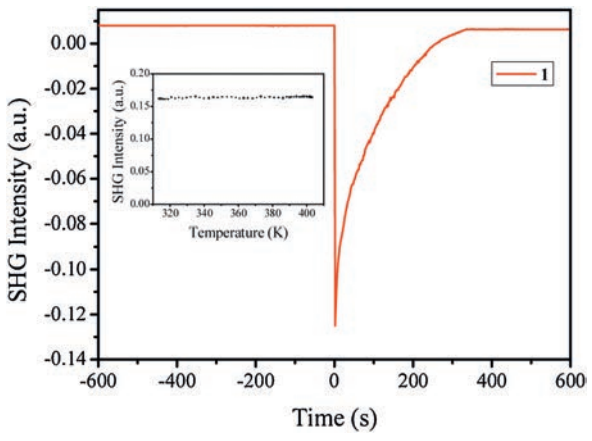

Fig. 3. Oscilloscope traces of SHG signals for **1** (λ = 1064 nm). Inset: the curve of variable temperature SHG.

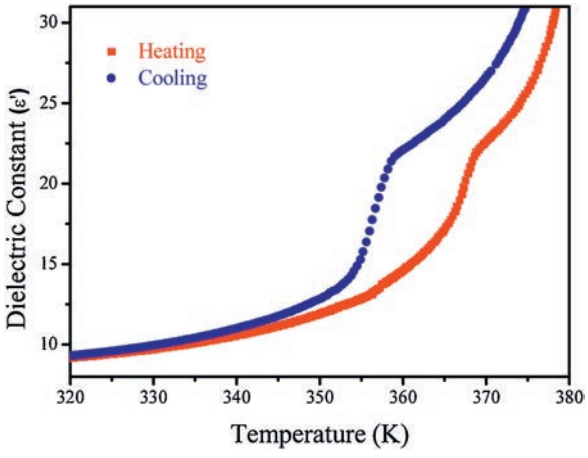

Fig. 4. Temperature-dependent dielectric constant of the polycrystalline sample of compound **1** at 1 MHz in the heating–cooling cycle.

temperature state, showing a significant change. It is obvious that the dielectric constant of **1** is always significantly changed near the phase transition temperature, which indicates that the dielectric measurement is a simple and effective method for detecting the occurrence of a phase transition. In addition, the dielectric loss can be compared with the dielectric constant to further verify the reversible phase transition. As shown in Fig. S8 (Supporting information), the dielectric loss ($\tan\delta$) displayed abnormal behavior with increasing temperature, corresponding to ε', confirmed the reversible phase transition.

In addition, the ε' curve shows a dielectric switch whose position is at the high temperature (Fig. 4). Around T_c, as the crystals undergo a high-temperature phase transition, ε' jumps into the range of 21.8–22.5, which corresponds to the dielectric switching behavior. As the temperature changes periodically, the intensity of the dielectric signal remains almost constant after nine cycles (Fig. S9 in Supporting information). These key results illustrate that the switch made of compound **1** has higher stability than other switching systems. It is worth mentioning that this switch further ascertains the occurrence of reversible phase transition. Provided that the low dielectric state at normal temperature is expressed as "off" and the high dielectric state at high temperature is indicated as "on", then when $T > T_c$ (phase transition temperature), the device is turned on, when $T < T_c$, the machine is turned off. Therefore, an excellent switch is formed between high temperature and normal temperature.

In summary, we have reported a new stimulus responsive switchable material, $[(CH_3)_3N(CH_2)_2Cl]_2[Mn(SCN)_4(H_2O)_2]$, which exhibits a high-temperature phase transition at 371 K with SHG effect. By substituting H with a halogen, the increased steric hindrance of the molecular make energy barrier increased, resulting in the reversible high-temperature phase transition. At the same time, the interactions of quasi-spherical cations and $[Mn(SCN)_4(H_2O)_2]^{2-}$ anions affect a non-centrosymmetric structure to induce the SHG effect. These findings throw light on the search for functional materials having both dielectric switch and second harmonic generation (SHG). Given that intelligent response and information processing have become crucial issues related to humankind life and daily production, there is no doubt that the stimulus response material $[(CH_3)_3N(CH_2)_2Cl]_2[Mn(SCN)_4(H_2O)_2]$ may be a potential candidate that could find applications in various fields such as optoelectronic equipment, data communications, actuators, memories, sensors and capacitors.

Declaration of competing interest

The authors declare that they have no known competing financial interests or personal relationships that could have appeared to influence the work reported in this paper.

Acknowledgments

This work was supported by the National Natural Science Foundation of China (Nos. 21673038, 21771037, 21805033), Natural Science Foundation of Jiangsu Province (JSNSF, No. BK20170659). Also we will gratefully appreciate the reviewers for their helpful discussion and constructive suggestions on the substantial improvement in the quality of the work.

Appendix A. Supplementary data

Supplementary material related to this article can be found, in the online version, at doi:https://doi.org/10.1016/j.cclet.2020.02.005.

References

[1] S.H. Baek, H.W. Jang, C.M. Folkman, et al., Nat. Mater. 9 (2010) 309.
[2] M. Salinga, M. Wuttig, Science 332 (2011) 543.
[3] M. Wuttig, N. Yamada, Nat. Mater. 6 (2007) 824–832.
[4] T. Akutagawa, H. Koshinaka, D. Sato, et al., Nat. Mater. 8 (2009) 342.
[5] S. Han, X. Liu, Y. Liu, et al., J. Am. Chem. Soc. 141 (2019) 12470–12474.
[6] H.Y. Ye, Y.Y. Tang, P.F. Li, et al., Science 361 (2018) 151.
[7] H.Y. Zhang, Z. Wei, P.F. Li, et al., Angew. Chem. Int. Ed. 57 (2018) 526–530.
[8] Y.M. You, Y.Y. Tang, P.F. Li, et al., Nat. Commun. 8 (2017) 14934.
[9] C.R. Bowen, H.A. Kim, P.M. Weaver, S. Dunn, Energy Environ. Sci. 7 (2014) 25–44.
[10] B. Champagne, A. Plaquet, J.L. Pozzo, V. Rodriguez, F. Castet, J. Am. Chem. Soc. 134 (2012) 8101–8103.
[11] B. Huang, J.Y. Zhang, R.K. Huang, et al., Chem. Sci. 9 (2018) 7413–7418.
[12] L. Li, X. Liu, Y. Li, et al., J. Am. Chem. Soc. 141 (2019) 2623–2629.
[13] H.T. Wang, L.H. Kong, P.P. Shi, et al., Chin. Chem. Lett. 26 (2015) 382–386.
[14] Y. Ai, X.G. Chen, P.P. Shi, et al., J. Am. Chem. Soc. 141 (2019) 4474–4479.
[15] M.A. Garcia-Garibay, Proc. Natl. Acad. Sci. U. S. A. 102 (2005) 10771.
[16] J. Harada, M. Ohtani, Y. Takahashi, T. Inabe, J. Am. Chem. Soc. 137 (2015) 4477–4486.
[17] Z.X. Zhang, T. Zhang, P.P. Shi, et al., J. Phys. Chem. Lett. 10 (2019) 4237–4244.
[18] L.H. Kong, D.W. Fu, Q. Ye, et al., Chin. Chem. Lett. 25 (2014) 844–848.
[19] P.F. Li, W.Q. Liao, Y.Y. Tang, et al., J. Am. Chem. Soc. 139 (2017) 8752–8757.
[20] W.Q. Liao, Y.Y. Tang, P.F. Li, Y.M. You, R.G. Xiong, J. Am. Chem. Soc. 140 (2018) 3975–3980.
[21] P.P. Shi, Y.Y. Tang, P.F. Li, et al., Chem. Soc. Rev. 45 (2016) 3811–3827.
[22] G.C. Xu, X.M. Ma, L. Zhang, Z.M. Wang, S. Gao, J. Am. Chem. Soc. 132 (2010) 9588–9590.
[23] T.T. Sha, Y.A. Xiong, Q. Pan, et al., Adv. Mater. 31 (2019) 1901843.
[24] P.P. Shi, S.Q. Lu, X.J. Song, et al., J. Am. Chem. Soc. 141 (2019) 18334–18340.
[25] A. Stroppa, P. Barone, P. Jain, J.M. Perez-Mato, S. Picozzi, Adv. Mater. 25 (2013) 2284–2290.
[26] Z. Wu, X. Liu, C. Ji, et al., J. Am. Chem. Soc. 141 (2019) 3812–3816.
[27] W.J. Xu, P.F. Li, Y.Y. Tang, et al., J. Am. Chem. Soc. 139 (2017) 6369–6375.
[28] Y.M. You, W.Q. Liao, H.Y. Ye, et al., Science 357 (2017) 306–309.
[29] H.Y. Zhang, Y.Y. Tang, P.P. Shi, R.G. Xiong, Acc. Chem. Res. 52 (2019) 1928–1938.
[30] W.Q. Liao, Y.Y. Tang, P.F. Li, Y.M. You, R.G. Xiong, J. Am. Chem. Soc. 139 (2017) 18071–18077.
[31] X.N. Hua, W.Q. Liao, Y.Y. Tang, et al., J. Am. Chem. Soc. 140 (2018) 12296–12302.
[32] W.Y. Zhang, Q. Ye, D.W. Fu, R.G. Xiong, Adv. Funct. Mater. 27 (2017) 1603945.
[33] H. Zhang, X. Wang, B.K. Teo, J. Am. Chem. Soc. 118 (1996) 11813–11821.
[34] Q. Li, P.P. Shi, Q. Ye, et al., Inorg. Chem. 54 (2015) 10642–10647.
[35] W.J. Xu, Z.Y. Du, W.X. Zhang, X.M. Chen, CrystEngComm 18 (2016) 7915–7928.